

# **Elastic Response and Failure Studies of Multi-wall Carbon Nanotube Twisted Yarns**

Thomas S. Gates  
Gail D. Jefferson  
Sarah-Jane V. Frankland

**American Society for Composites—Twenty-Second Technical Conference  
Seattle, WA, September 17 -19, 2007**

## **ABSTRACT**

Experimental data on the stress-strain behavior of a polymer–multiwall carbon nanotube (MWCNT) yarn composite are used to motivate an initial study in multi-scale modeling of strength and stiffness. Atomistic and continuum length scale modeling methods are outlined to illustrate the range of parameters required to accurately model behavior. The carbon nanotubes yarns are four-ply, twisted, and combined with an elastomer to form a single-layer, unidirectional composite. Due to this textile structure, the yarn is a complicated system of unique geometric relationships subjected to combined loads. Experimental data illustrate the local failure modes induced by static, tensile tests. Key structure-property relationships are highlighted at each length scale indicating opportunities for parametric studies to assist the selection of advantageous material development and manufacturing methods.

## **INTRODUCTION**

Since their discovery in 1991 [2] carbon nanotubes have sparked the imagination of many research groups around the world [3]. Carbon nanotubes can be found in several distinct formations including single-wall, double-wall, and multi-wall [4]. Recently, Baughman's group at University of Texas has developed a method for spinning carbon multi-wall nanotubes (MWCNTs) into a continuous yarn structure. This process is amenable to standard textile manufacturing techniques and allows for variation in the number of strands, number of plies, and geometric factors such as twist and yarn diameter [5], [6]. It is the objective of this paper to consider a yarn structure and to explore the atomistic and continuum relationships available to describe the elastic modulus and initial strength of this novel material system. This paper will highlight several key modeling challenges and outline the parameters of interest for textile modeling. Experimental data from recent tests by the authors will be presented to illustrate the similarity of MWNT yarns and natural fiber yarns.

As presented in Gates [7], traditionally, research institutions have relied on a discipline-oriented approach to development and design with new materials. It is recognized, however, that within the scope of materials and structures research, the breadth of length scales may range more than twelve orders of magnitude, and different scientific and engineering disciplines are involved at each level. Investigation of the mechanical response of the MWCNT yarn material may require material level descriptions that span at least six orders of length scale. As outlined in this paper, the yarn is a structural construct that exhibits properties that are functions of precursor material, loading conditions, and manufacturing induced helical geometry.

Most approaches to multiscale modeling are viewed as either bottoms up or top-down. Ultimately, the objectives of these two approaches, providing predictive methods for bulk behavior and guiding materials synthesis, are the same, but the methods, techniques, and the cross-scale handshaking is dictated by the approach. Ideally, both approaches should provide a two-way path for passing intrinsic, critical information across the scales. It is the former approach, bottoms-up, that will be the focus of this paper. The underlying assumption is that the intrinsic, critical structure and constitutive relationships developed at each scale are passed to the next scale with a well defined handshaking method. One of the difficulties associated with this assumption is that the information passed through the handshake should retain the detail and complexity needed to ensure accuracy. The approach considered in this paper requires a handshake but does not require direct coupling of computational methods. This approach contrasts with explicitly coupled models where full atomistic or molecular scale information is retained in a few, preassigned critical regions of the material, and higher scale continuum models are then used to model deformation in regions of the material that are more remote from the atomistic region [8].

## **MATERIALS**

The subject material test at NASA Langley Research Center is a yarn-elastomer composite. The composite is composed of a silicone rubber (Silicones, Inc GI1000) polymer with a single layer of embedded, aligned, four-ply MWCNT yarn fibers. Figure 1 provides a photograph of a cross-section of a typical test coupon.

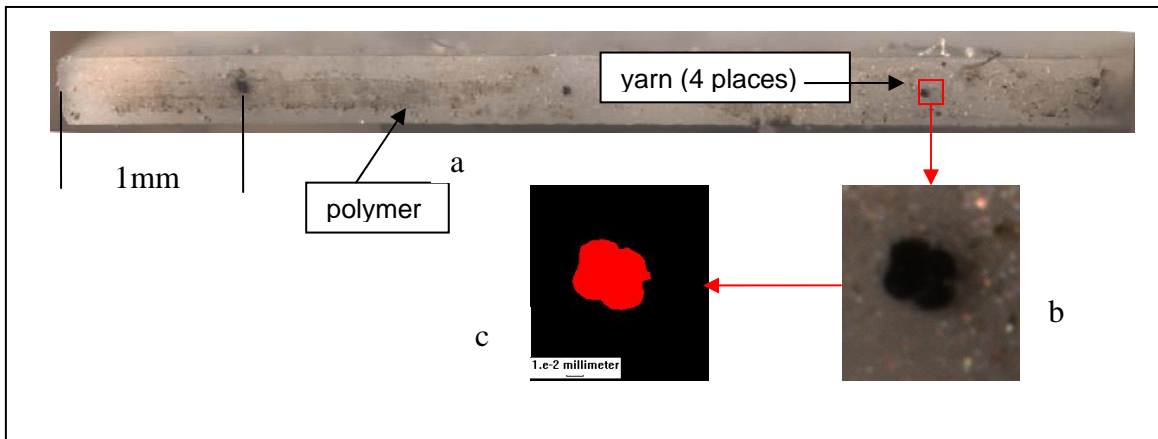


**Figure 1. a)Optical micrograph of a typical uniaxial tensile test coupon gage cross-section. b) Inset of right-most yarn on edge. c) Pictorial representation of area fraction of inset (~75% polymer).**

The precursor to the yarn structure is the MWCNT. The yarn material was supplied by Professor Ray Baughman, University of Texas at Dallas. The MWCNT yarn is created by simultaneously drawing and clockwise twisting (20 turns/mm) vertically aligned MWCNTs from a MWCNT forest to form a single yarn. Four of these singles are then twisted counterclockwise (4 turns/mm) forming a 4-ply yarn (Figure 2). The MWCNT yarn is similar in many respects to standard textile materials [9], and can be viewed as a unique structure whose properties are dependent not only on the precursor material (MWCNTs) but on yarn geometry and manufacturing methods. Additional details on the yarn and the associated properties can be found in [10], [11], and [12].

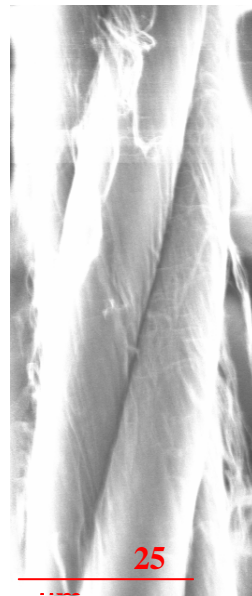


**Figure 2. SEM micrograph of a longitudinal view of typical four-ply multi-wall carbon nanotube yarn (2500x; 15kV).**

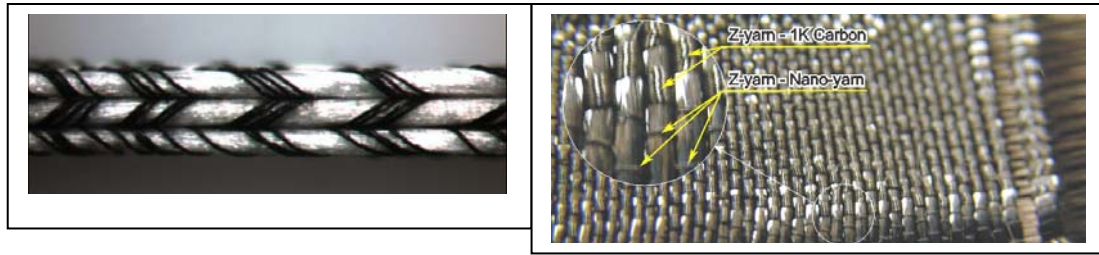


**Figure 3.** SEM photomicrograph of a hybrid glass fiber 3-D braid with CNT yarns visible as dark lines (left picture), and a 3-D woven fabric with 25-ply CNT yarns incorporated as the first five Z-yarns from the bottom (right figure). Ref. Bradford [1].

The MWCNT yarn can also be used in higher complexity forms such as the 3-D braid and woven fabric shown in Figure 3. In terms of length scales for the yarn structure under consideration, the following approximate structure-length relationships are assumed: MWCNT( $10^{-9}$  m), fibers( $10^{-7}$  m), single yarn( $10^{-6}$  m), yarn plies( $10^{-3}$  m). In this section of the paper, both atomistic and continuum mechanics approaches will be considered. The intent is to provide an initial review of methods available to calculate critical parameters for prediction of stiffness and strength.

### Molecular Level Simulations

The basic unit of the yarn is the MWCNT. In order to investigate the deformation and forces on a bundle of nanotubes, molecular dynamics simulations were performed of a system of (10,10) single-walled carbon nanotubes. Each nanotube contained 880 carbon atoms per 5.425 nm length. The nanotubes were simulated in a periodic box which contained 9 nanotubes (Figure 4). Each nanotube was represented with the Brenner-Tersoff potential [13]. The intra-nanotube interactions were modeled with the Lennard-Jones potential. The box was subjected to compression in the transverse x and y- directions. No change was made to the z-dimensions. The percent of deformation relative to the starting configuration is included in Table 1. Altogether, five levels of compression were simulated up to 15%.

At each level of compression strain, two simulations were performed. The first was carried out under equilibrium NVE conditions and the force on one of the nanotubes (Figure 4) was calculated in the direction normal to the nanotube surface. In the second simulation the same nanotube was loaded incrementally with axial force on each atom until the nanotube began to slide. Both the velocity of the nanotube and the distance that it traveled were monitored throughout the simulation. Two definitions were used to determine the initiation of nanotube axial motion. In the first the nanotube velocity was consistently positive above the thermal induced velocity fluctuations. In the second definition the nanotube was considered to be moving when it had traveled for 0.2 nm. The friction coefficient is calculated as the negative of the ratio of the applied to the normal load and is presented in Table 2. As explained in the following discussion. The normal load and apparent friction between nanotubes in a bundle may prove to serve as a starting point for macro-scale calculations of yarn fiber friction, a quantity that plays a role in both strength and stiffness calculations.

Table 1. Stress on the Nanotube System under Compression

Percent Compression (Nominal)	Stress Component in Transverse or x-direction (GPa)	Stress Component in Axial or z-direction (GPa)
0.0	-0.18	-0.04
2.0	1.73	0.80
5.0	1.77	0.97
10.0	1.86	1.24
15.0	1.89	1.64

Table 2. Apparent Friction Coefficient for Nanotubes Sliding.

Percent Compression	Method of Determining Pull-Through Force	Pull-Through Force (pN/atom)	Normal Force (pN/atom)	Apparent Friction Coefficient
0.0	velocity	0.053	-0.277	0.190
	distance	0.065		0.230
2.0	velocity	0.120	-8.40	0.015
	distance	0.120		0.014
5.0	velocity	0.075	-9.00	0.0083
	distance	0.068		0.0075
10.0	velocity	0.083	-5.40	0.015
	distance	0.081		0.015
15.0	velocity	0.043	-4.930	0.0088
	distance	0.030		0.0060

During compression of the nanotubes system, the relationship between the stress in the transverse direction and the normal load on the nanotube is non-linear. This non-linearity is not surprising because the nanotubes deform under compression.

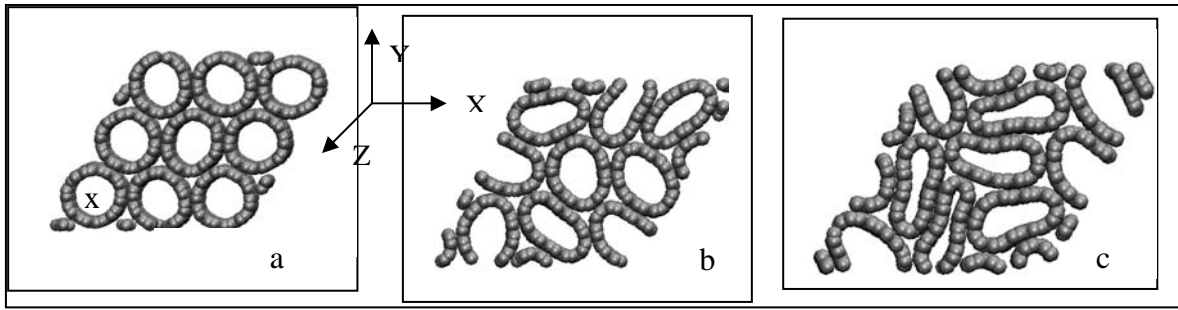


**Figure 4. Molecular structures of carbon nanotubes simulated with and with out transverse compression. (a) zero compression (b) 5% and (c) 15% compression. The marked nanotube (x) was loaded in the axial direction.**

The calculated friction coefficient decreases relative to the undeformed system as the system is compressed. The primary reason for this is that the normal force on the nanotube is also decreasing. The pull-out force initially increases at 2% compression then reduces with increasing compression. It is expected that during scale-up to the mechanics methods that the normal force on the nanotubes could be related to lateral forces induced under twist and axial load of a single yarn.

The polymer-yarn-nanotube interfaces have yet to be fully explored so it is worth noting that a nanotube sliding on a non-smooth surface such as the inside of a functionalized outer nanotube shows different friction characteristics than when it slides on a smooth surface. When the outer nanotube is not functionalized, the inner one slips easily in the axial direction. Therefore, the nanotube has a low friction coefficient in the non-functionalized case. When the outer nanotube is functionalized, the (absolute value) magnitude of the normal force is much smaller than the non-functionalized case, and inner one ‘sticks’ while trying to move axially within the rough surface of the outer nanotube. Both of these changes in the nanotube physical behavior raise the nanotube friction by at least two orders of magnitude. As demonstrated by others, [14], additional changes to nanotube sliding behavior occurs when there are defects in the outer nanotube or covalent bonding between nanotubes in MWCNTs. As described by Frankland [13], investigations of the composite should also consider covalent bonding of the nanotubes to the polymer.

At the atomistic scale, MD simulations by Qian [15] were used to estimate the load transferred to the central nanotube as a nanotube bundle of seven nanotubes is twisted. The simulation calculates the transferred load in the bundle versus the twist angle from 0-210 degrees. At zero degrees, a force of 0.048 eV/Å is transferred. At 120 degree the transferred load peaks at 1.63 eV/Å. For the current MWCNT yarn structure, the degree of twist of nanotubes at the nanoscale is expected to be small relative to the overall yarn twist. For the twisted bundle of fibers, it is assumed that the behavior of interest is directly related to the yarn twist and load-induced lateral compression that occurs at several length scales.

## Macro-level analysis

At the continuum mechanics scale, a large part of the relevant textile literature deals with dry single yarns, i.e. a yarn without any supporting matrix. A short review of several papers that describe dry yarn stress-strain behavior follows.

The complex geometry associated with twist and material variations implies that modulus of a yarn is a volume averaged structural property rather than a material property. This complexity results in both structure and axial load levels affecting all the mechanical properties of a twisted yarn. Generally, yarn twist is characterized by a twist multiplier (TM) [9].

$$TM = C^{1/2} \tau \quad (1)$$

Where  $\tau$  is the number of twists per unit length and  $C$  is the linear density with units of mass per unit length. During tensile loading of the yarn, the apparent stress-strain behavior will generally have a short linear region characterized by slippage of the fibers followed by nonlinearity with considerable extension while the fibers continue to slip and finally fiber failure occurs. During this axial loading of the yarn, off-angle forces in the yarn are generated by yarn twist. This multiaxial load state consists of combinations of axial tension and lateral compression.

Rao and Farris [16] considered the effects of material anisotropy on twisted yarns. They assumed that the yarn was composed of a series of thin-walled layers that resembles a unidirectional composite. The layers are located at a radial position ( $r$ ) in a yarn of radius ( $R$ ). The location of the filament is further defined by the angle ( $\theta$ ) between the single filament at  $r$  and the yarn major axis. Further, angle ( $\alpha$ ) is the angle ( $\theta$ ) at radius  $R$ . The apparent Young's modulus of a twisted yarn is calculated from the following expression

$$\hat{E} = \frac{2}{\tan^2 \alpha} \int_0^\alpha \frac{1}{S_{11}} \tan \theta \sec^2 \theta d\theta \quad (2)$$

where  $S_{11}$  is the principal compliance in the plane of a single transversely isotropic layer. If one assumes low twist and  $\alpha < 15^\circ$  then Rao arrives at an expression for the apparent Young's modulus of the yarn.

$$\hat{E} = E_z \left[ \left( \frac{3T_o + 1}{2dT_o} \right) + \frac{(1-d)^2}{d^3 \tan^2 \alpha} \ln \frac{(1-d)T_o + d}{T_o} \right] \quad (3)$$
$$d = \frac{E_z}{E_s}, \quad T_o = \cos^2 \alpha$$

The terms  $E_z$  and  $E_s$  are the longitudinal and shear modulus respectively of the fibers.

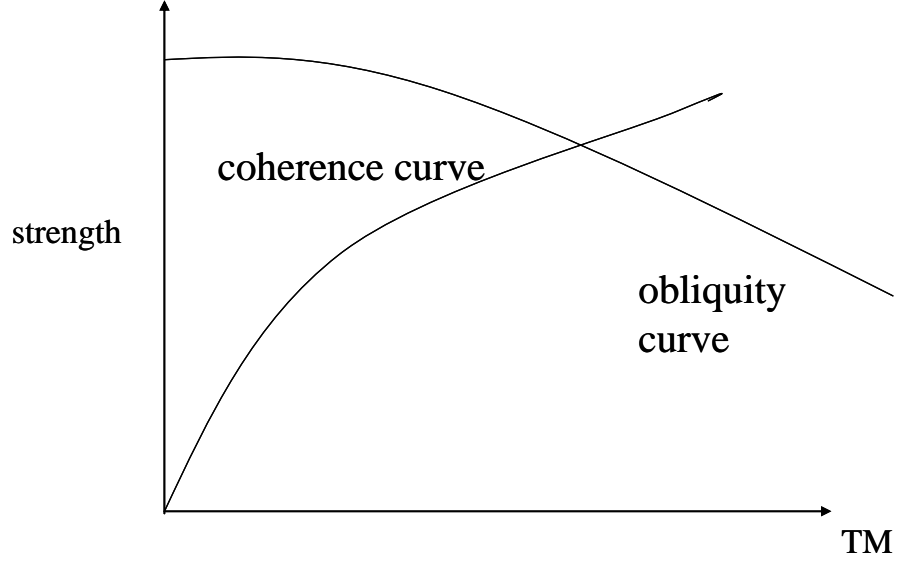


**Figure 5. Schematic representation of relationship of coherence, obliquity, and twist to yarn strength.**

Yarn strength has been found to be a function coherence (the degree of fiber packing) and obliquity (degree of order or parallelism of the fibers in the yarn). These basic relationships are visualized in the following schematic representation.

Considering yarn strength, there is an “optimum” twist associated with maximum strength of the yarn. Below this optimum, the yarn will fail due to fiber slippage while above the optimum; the yarn will fail by fiber fracture. As presented by Pan [17], [18] as a consequence of the lateral compression forces on the yarn, the yarn behaves as a chain of independent fragments. Each fragment is an individual due to fiber non-uniformity and specific fragment length. During yarn extension, fiber breakage continues until the length of the fiber fragment reaches a minimum dictated by the load carrying capability, or strength, of the fragment. This minimum length can be considered the “critical length” for this structure. The critical length has also been shown to decrease with increasing lateral pressure. Twist of the fiber and yarn diameter also plays a role in determining critical length although it is thought that twist improves the strength of high-performance fibers but decreases the strength of low-performance fibers [16].

Based on statistical interpretation of experimental data, Pan has proposed the following strength relationship.

$$\frac{\sigma_y}{\sigma_b} = \left( \frac{l_f}{l_c} \right)^{1/\beta} v_f \eta \quad (4)$$

Where  $\sigma_y$  is the yarn strength,  $\sigma_b$  is the fiber bundle strength,  $l_f, l_c$  are the fiber length and critical length respectively,  $v_f$  is the volume fraction of packing density of the yarn, and  $\beta, \eta$  are the Weibull shape parameter and orientation



efficiency factor respectively. An expression for the critical length of a yarn was presented by Realff [19]

$$l_c = \frac{2T_f}{\pi d \mu \sigma_l} \quad (5)$$

Where,  $T_f$  is the fiber tensile force at yarn fracture,  $d$  is the yarn diameter,  $\sigma_l$  is the lateral pressure, and  $\mu$  is a frictional coefficient. Realff [19] also presented this expression but asserted that contrary to Hearle [20], twist induced lateral pressure raises the overall strength of a yarn by increasing the apparent strength of the fibers.

Investigations by Gosh [21], [22] have demonstrated yarn mechanical behavior for a variety of material systems. Their studies have highlighted the influence of the helical geometry of the twisted yarn and the role of the resultant multiaxial forces generated during yarn axial tension by the unique structural arrangement of the fibers. Based upon test observations, they have proposed the following empirical expression for yarn tenacity.

$$Q = \frac{n_h}{n_e} F_h \frac{\mathcal{G}_b}{100} \cos^2 \theta \quad (6)$$

Where the terms of equation (6), defined below, are determined from test and observation. The concepts of yarn tenacity and the relationships to stress can be found in [20].

$n_h$  = number of fibers at location of yarn break

$n_e$  = average number of fibers in yarn cross-section

$n_h = n_e - 1.96\sigma$

$\sigma$  = standard deviation for 95% confidence level of number of fibers in yarn cross-section

$F_h$  = fiber bundle tenacity at gage length

$\theta$  = average helix angle of fibers in yarn failure zone

$\mathcal{G}_b$  = percent of broken fibers in yarn failure zone

Experimental evaluation of the nanotubes-polymer composite, described in the Materials section, reveals yarn stress-strain behavior in the composite similar to stress-strain behavior of a single dry fiber. The four-yarn polymer composite used in this study was subjected to uniaxial tension in a test stand with load measured using a standard load cell calibrated to +/-10N. Stress is engineering stress based on the load cell data and the average specimen cross-sectional area. The static tests are conducted with a small tensile preload and a constant displacement rate of 17mm/min for all the specimens. Once loaded to 50% of the gage length, the sample is unloaded at the same rate. Axial strain is calculated as the change in grip or crosshead displacement divided by the initial crosshead displacement as measured by the test machine's displacement transducer. Load and displacement data are collected at a rate of 2 samples/sec during the test using test machine's

digital data acquisition and control system. After the static tests were completed, the specimens are examined for local yarn failure characteristics such as location, mode and yarn-to-polymer interactions. Strain to failure levels in the polymer exceeded the designed limits of the test and consequently none of the composite specimens failed globally. In order to identify features at the nanoscale (type of fracture, interface characteristics, etc.) that will help provide insight into the failure of the yarn composite, optical and electron microscopy is performed after testing. Figure 6 provides some sample images of a cut and fractured yarn-polymer surface. Note the presence of polymer matrix in-between yarns in image 1 and the pull-out of the fractured yarn away from the surrounding polymer in images 2 and 3.

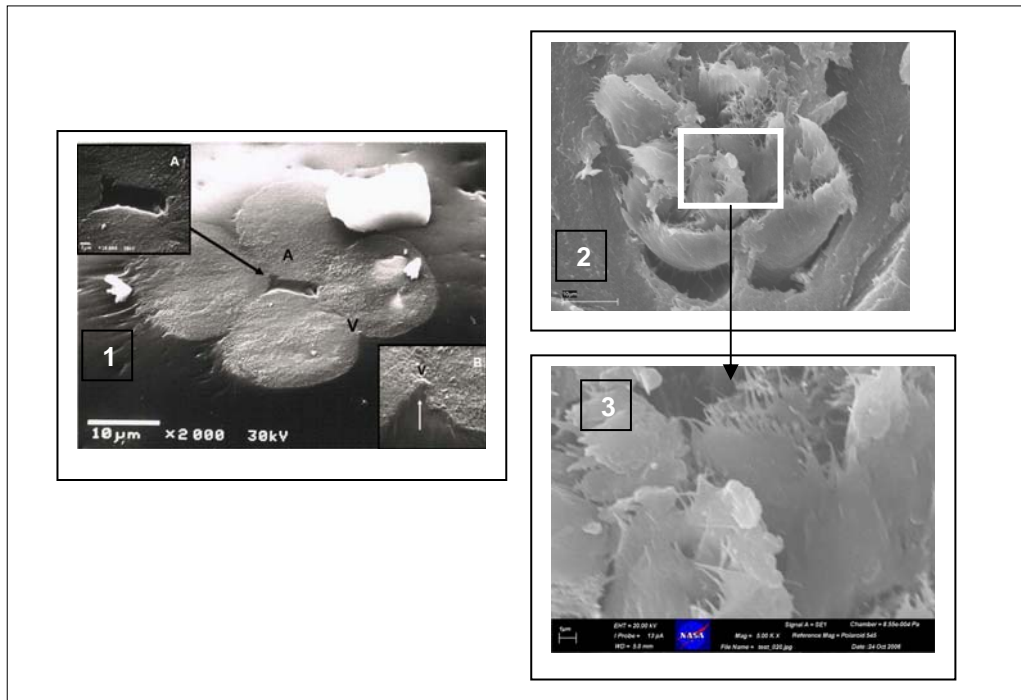


**Figure 6. SEM images of a four ply yarn. Image 1: cut surface [23]. Image 2: Fractured surface. Image 3: Enlargement of fractured yarn.**

A representative stress-strain curve for the static tensile test of the composite is provided in Figure 7. Upon loading, initial failure corresponds to the maximum stress (point 3). At initial failure, all five yarns failed simultaneously at the same location with respect to the longitudinal axis (Figure 8). The majority of test specimens had initial failure occur in the gage section. Upon further loading, the specimen has lost stiffness but continues to carry load until the stress reaches the secondary failure level (point 5). At this point simultaneous failure of all five yarns occurs again but at a location different from the point of initial failure. As the yarn fails in distinct segments, the effective stiffness of the composite trends toward the stiffness of the polymer matrix. Finally, upon unloading, the specimen does not return to its initial configuration (point 8).

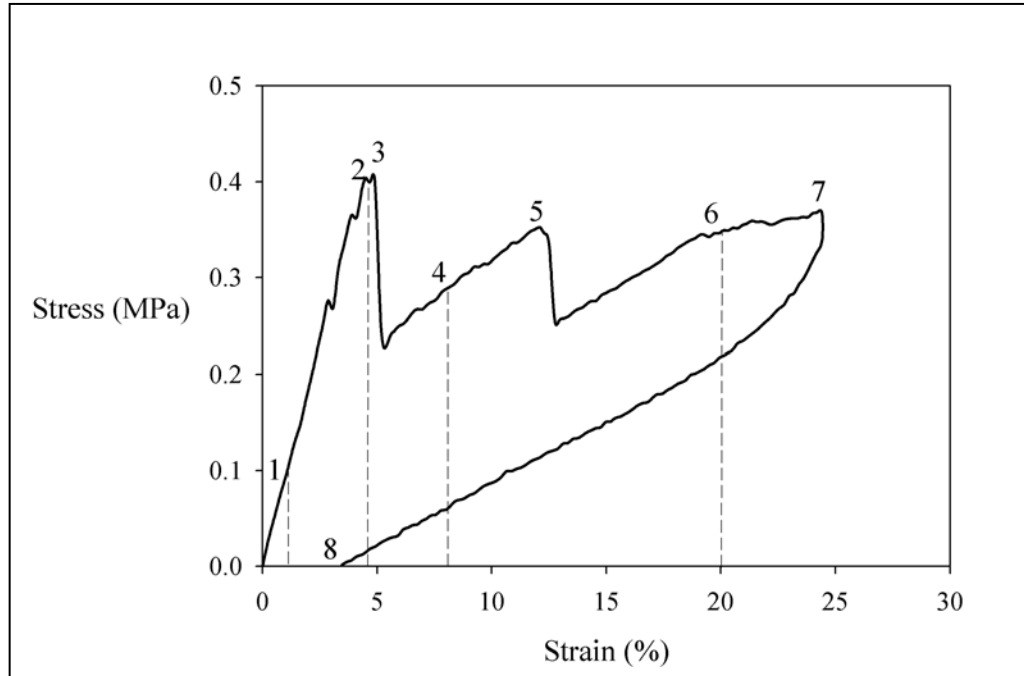


**Figure 7. Representative Engineering Stress - Strain curve for 5 yarn composite loaded in static tension. Note: 1 – 1% strain; 2 – 4.5% strain; 3 – first failure across all yarn; 4 – 8% strain; 5 – secondary failure; 6 – 20% strain; 7 – 50% gage length (point of unload); 8 – final strain**

At failure, the yarns did not pull-out from the matrix but did exhibit spring-back or recoil along the loading axis. This behavior is highlighted in Figure 8 by a series of photographs of a composite after failure. The failed yarns take on a resemblance to a buckled column structure on an elastic foundation. This type of behavior was also observed in [6]. Their explanation revolves around the model that predicts shear and compressive loads along the interface between yarn and matrix. These loads are due to differences in yarn and matrix longitudinal strains and lateral contractions. Yarn failure in Figure 7 was clearly defined and the post-mortem inspections revealed that the yarn breaks were even with each yarn single failing on the same cross-sectional plane. As illustrated in Figure 9, the buckled fiber contributes little to additional load carrying capacity of the composite. In addition, examining Figure 9, it is reasonable to contribute the regularity of the breaks and yarn segment lengths to the ideas behind the concepts of critical length as presented in equation(5).

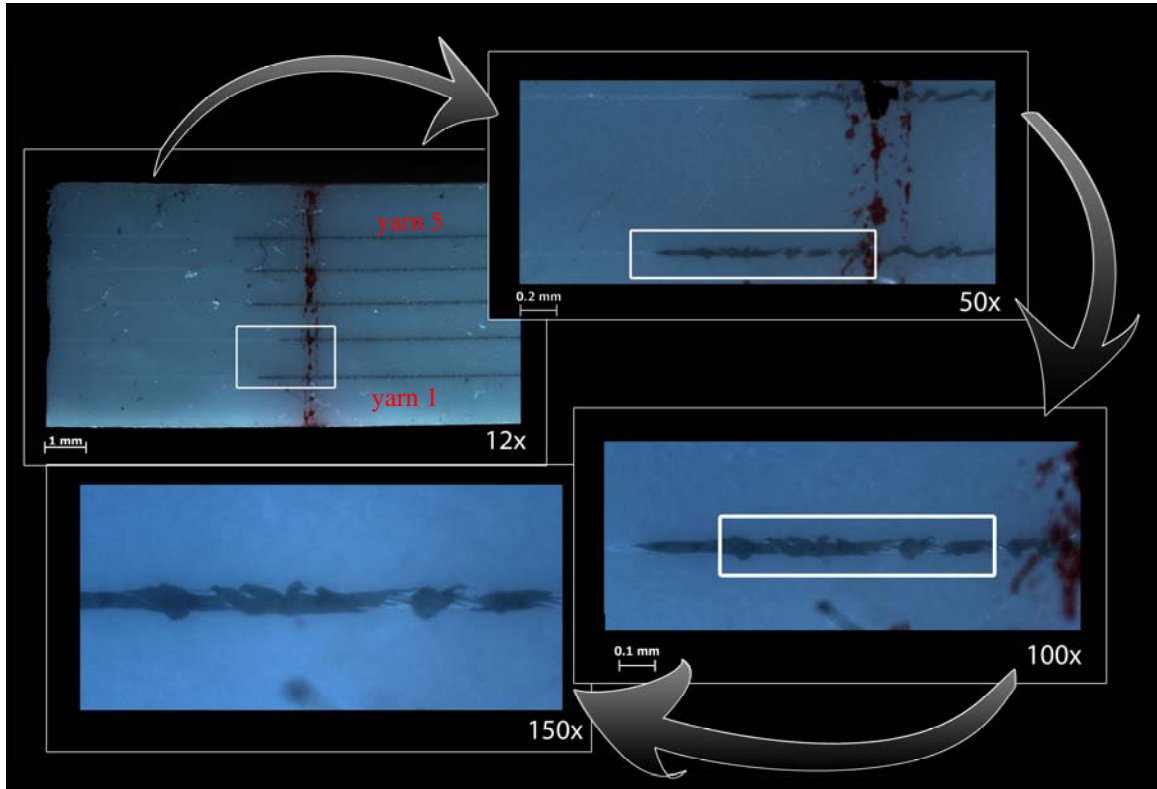


**Figure 8. Optical micrograph of failed tensile specimen gage section-longitudinal view. 12x – view of failure zone of all 5 yarns; 50x – inset of yarn 1 and yarn 2; 100x – inset of yarn 1; 150x – inset of yarn 1 and initial configuration of yarn 1. Note: Vertical red line denotes the center of the sample.**

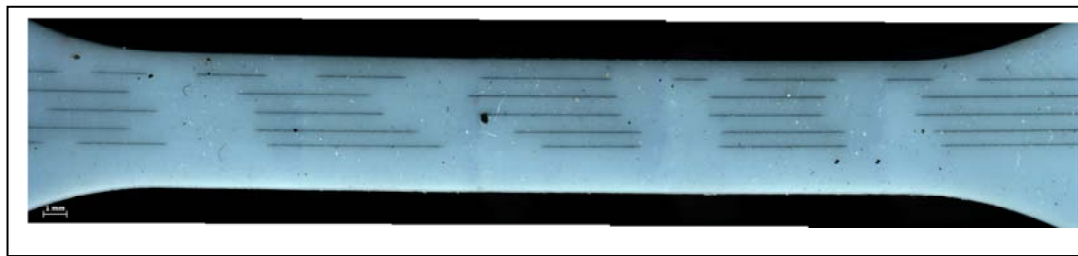


**Figure 9. Optical microphotograph (12x) of failed composite tensile specimen illustrating the sequence of yarn segments.**

## SUMMARY

A novel nanostructured composite material was considered as a candidate for multi-scale analysis of strength and stiffness. As discussed by [24] and [25], it is often the interface region that governs the material response. This is true for a range of properties including mechanical, electrical and thermal. The implication is that the multiscale analysis method must provide sufficient detail in the interface. Due to practical limitations on computational speed and size, the level of detail must be tempered against expediency and efficiency. The material interface requires a transition between scales and their associated methods. This paper presented an initial attempt to experimentally and analytically describe stiffness and strength of a MWCNT yarn-polymer composite.

The matrix material in the composite is an elastomer and the reinforcement is provided by five, four-ply multi-wall carbon nanotube yarns. The composite has a yarn volume fraction of 0.0028. An experimental study was performed to determine the static mechanical response of the multiwall carbon nanotube – polymer composite. Strength, stiffness, and failure were characterized for both the polymer and the composite loaded in uniaxial tension. The yarn response is dependent upon inherent material properties as well as yarn structure, geometry and manufacturing method. Despite the low yarn volume fraction, the composite modulus was increased by over a factor of ten compared to the base polymer. The composite exhibited linear elastic behavior up to initial failure. The high strain value (~5%) at failure resulted in catastrophic yarn failure with all yarns failing simultaneously at some characteristic length. Failure modes of the yarns were not unlike fabric yarn failure modes described in the textile literature. As is typical with twisted yarns, the final yarn structure or bundle does not retain the strength or stiffness of the base material or strands. The scale-up from MWCNT to the yarn implies the final yarn properties are a function of base material properties, material twisting, fiber migration, frictional forces and lateral compressive forces developed at each material level or length scale.

Due to the homogenization process, a set of assumptions accompanies each scale in the yarn structure including the interface transition regions. The solutions to multiscale analysis are material and application specific and transition between scales is the essential challenge. For a novel material such as the multi-wall carbon nanotube yarn, the solution to predicting mechanical behavior requires the coordinated contributions of engineering, science and computational expertise as well as the direct coupling of experimentation and modeling.

## REFERENCES

1. Bradford, P.D. and A.E. Bogdanovich, *Fabrication and Properties of Multifunctional, Carbon Nanotube Yarn Reinforced 3-D Textile Composites*, in *16th International Conference on Composite Materials*, 2007, Kyoto, Japan.
2. Iijima, S., *Helical Microtubes of Graphitic Carbon*, Nature (London), 1991, 354: pp. 56-58.
3. Lau, K.-T. and D. Hui, *The Revolutionary Creation of New Advanced Materials - Carbon Nanotube Composites*, Composites, Part B, 2002, 33: pp. 263-277.
4. Harris, P.J.F., *Carbon Nanotubes and Related Structures*, 1999, Cambridge: Cambridge University Press.
5. Bogdanovich, A., et al. *Fabrication and Mechanical Characterization of Carbon Nanotube Yarns, 3-D Braids, and Their Composites*, in *SAMPE Fall Technical Conference*, 2006, Dallas, TX.
6. Amirbayat, J. and J.W.S. Hearle, *Properties of Unit Composites as Determined by the Properties of the Interface. Part I: Mechanisms of Matrix-Fibre Load Transfer*, Fibre Science and Technology, 1969, 2(123).
7. Gates, T.S., G.M. Odegard, S.J.V. Frankland, and T.C. Clancy, *Computational Materials: Multiscale Modeling of Nanostructured Materials*, Journal of Composite Science and Technology, Anniversary Issue, 2005, 65/15-16: pp. 2416-2434.
8. Odegard, G.M., T.S. Gates, L.M. Nicholson, and K.E. Wise, *Equivalent-Continuum Modeling of Nano-Structured Materials*, Composites Science and Technology, 2002, 62(14): pp. 1869-1880.
9. Hearle, J.W.S., *Yarn Texturing Technology*, ed. W.P. Limited, 2000, Cambridge.
10. Dalton, A.B., et al., *Super-Tough Carbon-Nanotube Fibres*, Nature, 2003, 423 (723).
11. Zhang, M., K.R. Atkinson, and R.H. Baughman, *Multifunctional Carbon Nanotube Yarns by Downsizing an Ancient Technology*, Science, 2004, 306: pp. 1358-1361.
12. Zhang, M., et al., *Strong, Transparent, Multifunctional, Carbon Nanotube Sheets*, Science, 2005, 309(1215): pp. 1215-1219.
13. Frankland, S.J.V., C. A., B. D.W., and G. M., *Molecular Simulation of the Influence of Chemical Cross-Links on the Shear Strength of Carbon Nanotube-Polymer Interfaces*, J Phys Chem B, 2002, 106: pp. 3046-3048.
14. Huhtala, M., A.V. Krasheninnikov, and J. Aittoniemi, *Improved Mechanical Load Transfer between Shells of Multiwalled Carbon Nanotubes* Physical Review B, 2004, 70(4).
15. Qian, D., W.K. Liu, and R.S. Ruoff, *Load Transfer Mechanism in Carbon Nanotube Ropes* Composite Science and Technology, 2003, 63(11): pp. 1561-1569.
16. Rao, Y. and R.J. Farris, *A Modeling and Experimental Study of the Influence of Twist on the Mechanical Properties of High-Performance Fiber Yarns*, Journal of Applied Polymer Science, 2000, 77: pp. 1938-1949.

17. Pan, N., *Fiber Interactions in a Twisted Fiber Structure under Tension*, IEEE, 1996, 7803(3519): pp. 138-142.
18. Pan, N. and T. Hua, *Relationship between Fiber and Yarn Strength*, Textile Research Journal, 2001, 71(11): pp. 960-964.
19. Realff, M.L., et al., *A Stochastic Simulation of the Failure Process and Ultimate Strength of Blended Continuous Yarns*, Textile Research Journal, 2000, 70(5): pp. 415-430.
20. Hearle, J.W.S., P. Grosberg, and S. Backer, *Structural Mechanics of Fibers, Yarns, and Fabrics*, Vol. 1, 1969, New York: Wiley-Interscience.
21. Ghosh, A., S.M. Ishtiaque, and R.S. Rengasamy, *Analysis of Spun Yarn Failure, Part I: Tensile Failure of Yarns as a Function of Structure and Testing Parameters*, Textile Research Journal, 2005, 75(10): pp. 731-740.
22. Ghosh, A., S.M. Ishtiaque, and R.S. Rengasamy, *Analysis of Spun Yarn Failure, Part II: The Translation of Strength from the Fiber Bundle to Different Spun Yarns*, Textile Research Journal, 2005, 75(10): pp. 741-744.
23. Hernandez, C.D., et al. *Multifunctional Characteristics of Carbon Nanotube Yarns Composites*, in ASME, MN2006-17028, *Multifunctional Nanocomposites*, 2006, Honolulu Hawaii.
24. Wagner, G.J. and W.K. Liu, *Coupling of Atomistic and Continuum Simulations Using a Bridging Scale Decomposition*, J. Comput. Phys, 2003, 190: pp. 249–274.
25. Liu, W.K., et al., *Bridging Scale Methods for Nanomechanics and Materials*, Comput. Methods Appl. Mech. Engrg., 2006, 195: pp. 1407–1421.